

DEPOSITION AND CHARACTERIZATION OF Ti_{0.5}Al_{0.5}N/CrN MULTILAYER COATINGS SPUTTERED AT LOW TEMPERATURE

NANOS IN KARAKTERIZACIJA VEČPLASTNE PREVLEKE Ti_{0.5}Al_{0.5}N/CrN, NAPRŠENE PRI NIZKI TEMPERATURI

Peter Panjan, Miha Čekada, Darja Kek-Merl, Igor Urankar, Anton Zalar

¹Jožef Stefan Institute, Jamova 39, 1000 Ljubljana, Slovenia
peter.panjan@ijs.si

Prejem rokopisa - received: 2003-03-18; sprejem za objavo - accepted for publication: 2003-05-05

Ti_{0.5}Al_{0.5}N/CrN multilayer coatings were prepared using sputter deposition at a low deposition temperature. This particular multilayer was chosen because it provides a combination of the attractive properties of Ti_{0.5}Al_{0.5}N and CrN single-layered coatings. The PVD multilayered Ti_{0.5}Al_{0.5}N/CrN coatings on HSS were evaluated with respect to fundamental properties such as morphology, crystal structure, microhardness, adhesion and oxidation resistance. The microhardness and Young's modulus of the Ti_{0.5}Al_{0.5}N/CrN multilayered coatings were found to be slightly higher than those observed for single-layered coatings, while other properties (internal stress, oxidation resistance) were halfway between the CrN and the TiAlN coatings. The ball-crater technique used on the scratch tracks showed that the Ti_{0.5}Al_{0.5}N/CrN multilayer structure has a higher cracking resistance than the TiAlN and the CrN.

Keywords: Hard coatings, PVD, Multilayer Ti_{0.5}Al_{0.5}N/CrN coating

Večplastno strukturo Ti_{0.5}Al_{0.5}N/CrN smo pripravili z reaktivnim naprševanjem pri nizki temperaturi. To prevleko smo raziskovali zato, ker združuje zanimivo kombinacijo lastnosti prevlek Ti_{0.5}Al_{0.5}N in CrN. Preiskovali smo nekatere osnovne lastnosti večplastne prevleke Ti_{0.5}Al_{0.5}N/CrN, nanesene na podlage iz hitroreznega jekla, kot so kristalna struktura, morfologija, mikrotrdota, adhezija in oksidacijska odpornost. Ugotovili smo, da sta mikrotrdota in Youngov modul večplastne strukture Ti_{0.5}Al_{0.5}N/CrN nekoliko večja od vrednosti za enojno plast TiAlN oz. CrN, medtem ko so nekatere druge lastnosti (notranje napetosti, oksidacijska obstojnost) neke vmes med tistimi za TiAlN in CrN. Iz krogelnega obrusa čez razo, narejeno z diamantno konico med meritvijo adhezije, smo ugotovili, da se v večplastni prevleki Ti_{0.5}Al_{0.5}N/CrN mikrorazpoke širijo teže kot v enojni prevleki TiAlN oz. CrN.

Ključne besede: trde prevleke, PVD, večplastna struktura Ti_{0.5}Al_{0.5}N/CrN

1 INTRODUCTION

Multilayer PVD hard coatings have been studied intensively over the past few years because of their promising properties¹⁻⁴. They have a number of advantages over single layers as they combine the attractive properties of several materials as well as exhibiting some completely new properties that are not observed with single layers. Each layer in such a multilayer structure contributes to the surface with some of its specific properties. Multilayered coatings have been found to possess better mechanical properties - for example, higher microhardness and fracture toughness, greater strength, elasticity and plasticity - than single-layer coatings. The benefits of multilayer coatings have been partly used in most of the CVD coatings used commercially today on an industrial scale. While CVD hard coatings are usually structures with up to 13 individual layers (TiC, TiN, Ti(C, N), Al₂O₃), PVD coatings can be prepared either with a limited number of single layers (e.g. Ti, TiN, TiC, CrN, NbN and Ti_{0.5}Al_{0.5}N) or with a very large number of single layers (up to 2000). The functional and structural properties as well as the performance of PVD multilayer coatings can

be tailored by selecting the material for the individual layers, adjusting the interface volume and constitution, and optimizing the individual layer sequence and thickness. The sputtering process seems to be the most suitable technique for the preparation of multilayer coatings.

A multilayer coating is more effective than a single layer for milling materials such as cast iron because it withstands the thermal shock load much better. It also performs very well in high-speed milling operations. As a result, commercial applications for some multilayer coatings were found in high-speed and dry-cutting operations (e.g. TiN/TiAlN - Balzers Futura, SUPER R-Dormer).

For the past ten years investigations have been concentrated on studying the deposition and properties of various multilayer and superlattice coatings based on nitrides and carbides of titanium, for example TiN/NbN, TiN/TiAlN, CrN/TiN, TiN/AlN, TiN/MoN, TiN/TaN, TiN/TiCN, TiC/TiCN/TiN, CrN/CrAlN, TiN/AlN and TiAlN/CrN⁵⁻¹³. However, only two studies relating to Ti_{0.5}Al_{0.5}N/CrN multilayer coatings exist^{7,8}. Luo et al⁷ reported a tribological investigation of Ti_{0.5}Al_{0.5}N/CrN coatings with superlattice characteristics grown by a

combined steered-arc/unbalanced magnetron deposition system. The same group⁸ also studied the thermal stability of such a structure.

We previously studied TiN/CrN multilayer structures deposited at a low temperature¹³. In this study PVD multilayered Ti_{0.5}Al_{0.5}N/CrN coatings on HSS were evaluated with respect to fundamental properties such as morphology, microstructure, microhardness, adhesion, fracture resistance and oxidation resistance. This particular multilayer was chosen because it provides a combination of the attractive properties of Ti_{0.5}Al_{0.5}N and CrN single coatings. While TiAlN coatings are used in dry and high-speed machining operations because of their high oxidation and abrasion resistance, CrN coatings can be used when better oxidation and corrosion resistance are needed.

2 EXPERIMENTAL

A 2.33- μm -thick coating was deposited by reactive sputtering in a Sputron (Balzers) plasma-beam-sputtering apparatus at a temperature below 150 °C on polished M2 high-speed tool-steel discs and alumina ceramics. The SPUTRON apparatus has four in-situ exchangeable targets, which makes it possible to prepare various kinds of multilayer structures under vacuum. Sequential sputtering was used to fabricate multilayer coatings with eight layers. The single layer thickness was 250-310 nm (**Figure 1**). Depth profile analyses of the as-deposited and oxidized Ti_{0.5}Al_{0.5}N/CrN multilayer coatings were carried out using a PHI SAM 545A Auger electron spectrometer. A microstructural study of the film was made using a JEOL JXA 840A scanning electron microscope (SEM). The phase and crystal structure of the as-deposited and oxidized coatings were identified with a Huber G600 thin-film diffractometer with Seeman-Bohlin (SB) geometry and a conventional PW 1710 Phillips diffractometer with Bragg-Brentano (BB) geometry. The coating adhesion was characterized with a conventional Revetest scratch tester (CSEM, loading rate 100 N/min, scratching rate 10 mm/min). Microhardness measurements were taken using a Mitutoyo MVK-H2 tester using 25 and 50 g loads. Each data point was determined from the mean of 30 separate measurements. Microhardness measurements were also performed with a Fischerscope H 100 and the microhardness and Young's modulus were calculated. The ball-cratering preparation technique (the diameter of the 100Cr6 steel ball was 20 mm, the diamond paste was 0.25 μm) and reflected-light microscopy were applied to measure the thickness of the individual layers, as well as to observe the deformation and fracture behaviour of the coatings on the scratch tracks. The oxidation of the coatings was carried out by heating the samples at temperatures of 800-900 °C in an oxygen atmosphere for selected times. The heat treatment was performed in a programmable process tube furnace. For the oxidation-

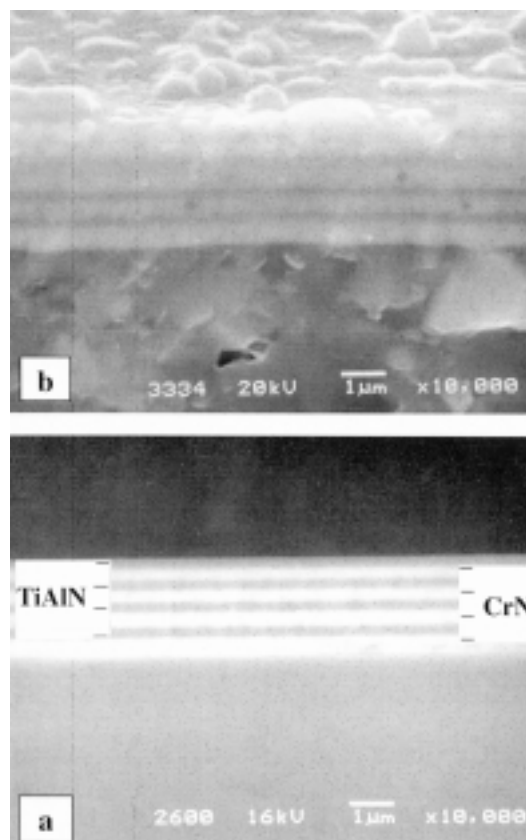


Figure 1: SEM backscattered electron micrographs of the fracture cross-section of a Ti_{0.5}Al_{0.5}N/CrN multilayer coating (a - as-deposited sample, b - sample oxidized at 850 °C for 1300 min)

Slika 1: Posnetek preloma večplastne strukture Ti_{0.5}Al_{0.5}N/CrN, narejen z vrstičnim elektronskim mikroskopom (a - vzorec po nanosu, b - vzorec, oksidiran pri 850 °C, 1300 min)

rate measurements polished alumina ceramics with roughness $R_a = 25$ nm were used as substrates. The samples were oxidized at high temperature and periodically taken out of the furnace to measure the weight gain using a precise microbalance (Mettler UM2).

3 RESULTS

The basic properties of the Ti_{0.5}Al_{0.5}N/CrN multilayer coating are given in **Table 1**. The corresponding properties of the Ti_{0.5}Al_{0.5}N and CrN single-layer coatings are added for comparison.

The chemical modulation period of the Ti_{0.5}Al_{0.5}N/CrN multilayer structure was determined from an SEM backscattered electron micrograph of a fractured cross-section (**Figure 1a**). The total thickness of the multilayer structure is 2.4 μm , while the thickness of the individual Ti_{0.5}Al_{0.5}N and CrN layers is 250 and 310 nm, respectively. The thickness of the individual layers can also be resolved from the ball craters using reflected-light microscopy (**Figures 2a,b**), as well as from the AES depth profile (**Figure 3**). AES was also

Table 1: Characteristics of PVD Ti_{0.5}Al_{0.5}N, CrN and Ti_{0.5}Al_{0.5}N/CrN coatings sputter deposited at low temperature. (*L_c(AE)* - the adhesion critical force for onset of acoustic emission, *L_c(F_t)* - adhesion critical force for scratching force jump, HV - microhardness, *E* - Young's modulus, *E_a* - activation energy for oxidation, *k_p* - parabolic constant of oxidation)

Tabela 1: Lastnosti prevlek Ti_{0.5}Al_{0.5}N, CrN in Ti_{0.5}Al_{0.5}N/CrN napršenih pri nizki temperaturi. (*L_c(AE)* - kritična sila, pri kateri se pojavi akustična emisija, *L_c(F_t)* - kritična sila, pri kateri se sila razenja skokovito poveča, HV - mikrotrdota po Vickersu, *E* - Youngov modul, *E_a* - aktivacijska energija za oksidacijo, *k_p* - parabolična konstanta oksidacije)

	CrN	Ti _{0.5} Al _{0.5} N/CrN	Ti _{0.5} Al _{0.5} N
Thickness (µm)	1.95	2.33	1.47
HV _{0.025} (Mitutoyo)	2048±137	2476±149	1681±127
HV _{0.05} (Mitutoyo)	1372±7	1663±102	951±40
HV _{0.01} (Fischerscope)	2873±93	3085±435	2099±253
HV _{0.05} (Fischerscope)	1347±17	1546±28	1180±4
<i>E</i> _{0.05} (GPa)	231±8	244±6	213±3
<i>L_c(AE)</i> (N)	26±9	62±11	46±5
<i>L_c(F_t)</i> (N)	52±10	70.5±10	82±13
Internal stress (MPa)	-490	-1390	-2500
<i>E_a</i> (eV)	2.1	3	3.8
<i>k_p</i> at 800 °C (µg ² /cm ⁴ min)	6.2	2.52	1.1
<i>k_p</i> at 900 °C (µg ² /cm ⁴ min)	73	23	4

used to determine the composition of the Ti_{0.5}Al_{0.5}N and CrN. All the coatings contained only very small amounts of oxygen and carbon (below 1 at%). Very sharp interfaces were observed between all the single layers.

The internal stress (σ) was calculated from the sample deflection using Stoney's formula for a circular specimen¹⁴:

$$\sigma = \frac{\delta E_s d_s^2}{3R^2(1-\nu_s)d_f}$$

where *E_s*, *ν_s* and *d_s* are the Young's modulus, the Poisson's ratio and the thickness of the substrate; *d_f* is the thickness of the film, *R* is the sample diameter and δ is the sample deflection. The sample deflection δ was measured by a Taylor-Hobson Talysurf 2 profilometer. The results of the internal stress measurement presented in Table 1 were normalized for coatings with a thickness of 3 µm. A low value of internal stress for the CrN coating was observed, while the values for the Ti_{0.5}Al_{0.5}N are much higher. The internal stress for the

Ti_{0.5}Al_{0.5}N/CrN coating was halfway between the CrN and Ti_{0.5}Al_{0.5}N coatings.

Figures 4 a, b shows BB and SB high-angle X-ray patterns for a multilayered sample. Both BB and SB spectra show only diffraction peaks, which can be indexed to the reflections of Ti_{0.5}Al_{0.5}N and CrN, and no satellite peaks around the (111) and (200) reflections appeared. XRD revealed a <111> texture in the Ti_{0.5}Al_{0.5}N/CrN coatings, while <200> texture was observed in the other two coatings.

The microhardness of all three coatings on the M2 high-speed tool steel was determined with a conventional Vickers tester (Mitutoyo MVK-H2). Thirty indentations were made at each load and the average hardness value and standard deviation were calculated. The microhardness of the Ti_{0.5}Al_{0.5}N/CrN was found to be slightly higher than that of the Ti_{0.5}Al_{0.5}N and CrN single layers of comparable total thickness (see Table 1).

The plastic-elastic properties of the coatings were estimated with a H 100 Fischerscope microindentation

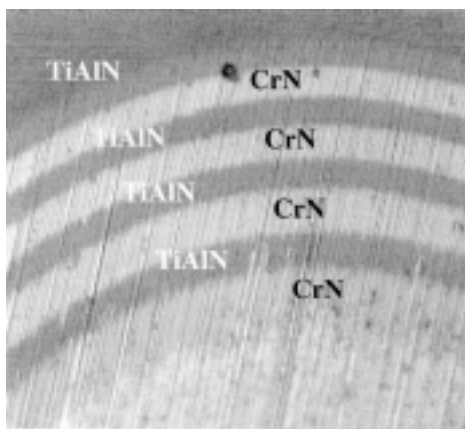


Figure 2: Reflected light micrograph of ball craters in an as-deposited Ti_{0.5}Al_{0.5}N/CrN multilayer coating with eight layers (mag. 400x)

Slika 2: Optičnomikroskopski posnetek obrusa prevleke v obliki večplastne strukture Ti_{0.5}Al_{0.5}N/CrN, ki je sestavljena iz 8 plasti

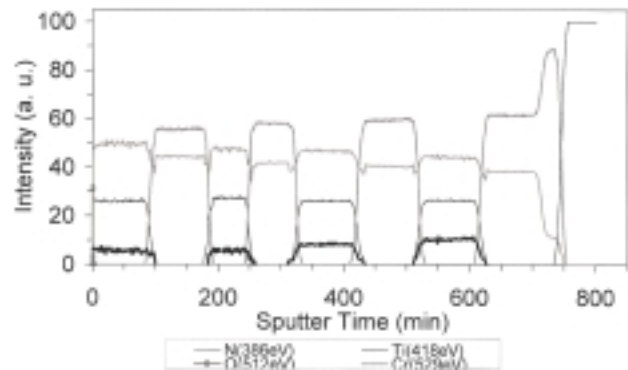


Figure 3: AES depth profiles of as-deposited and oxidized Ti_{0.5}Al_{0.5}N/CrN multilayer coatings deposited on a steel substrate.

Slika 3: Globinski AES-profil večplastne strukture Ti_{0.5}Al_{0.5}N/CrN po nanosu in oksidaciji

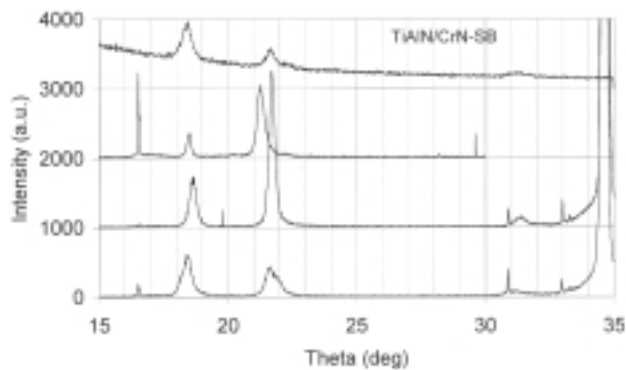


Figure 4: BB and SB X-ray diffraction patterns of a $\text{Ti}_{0.5}\text{Al}_{0.5}\text{N}/\text{CrN}$ multilayer coating. BB X-ray spectra of CrN and $\text{Ti}_{0.5}\text{Al}_{0.5}\text{N}$ are added for comparison.

Slika 4: Uklonski spektri BB in SB večplastne strukture $\text{Ti}_{0.5}\text{Al}_{0.5}\text{N}/\text{CrN}$. Za primerjavo sta dodana BB-spektra plasti CrN in $\text{Ti}_{0.5}\text{Al}_{0.5}\text{N}$.

device. The measurement was performed using a loading and unloading cycle. The indentation load was increased from 0.4 mN to 100 mN and from 0.4 mN to 500 mN, respectively. The hardness value is derived from the test load and the indentation surface area, which is derived from the indentation depth, while the Young's modulus is calculated by the slope of the initial portion of the unloading curve. Mean values were calculated based on 10 individual observations. The results presented in **Table 1** show that the $\text{Ti}_{0.5}\text{Al}_{0.5}\text{N}/\text{CrN}$ coating has a higher microhardness and Young's modulus than the CrN and $\text{Ti}_{0.5}\text{Al}_{0.5}\text{N}$ single layers.

Adhesion was evaluated by measuring the critical loads for the beginning of acoustic emission $L_c(\text{AE})$ and for a rapid increase in the scratching force $L_c(F_t)$, which corresponds to the total delamination of the coating. The

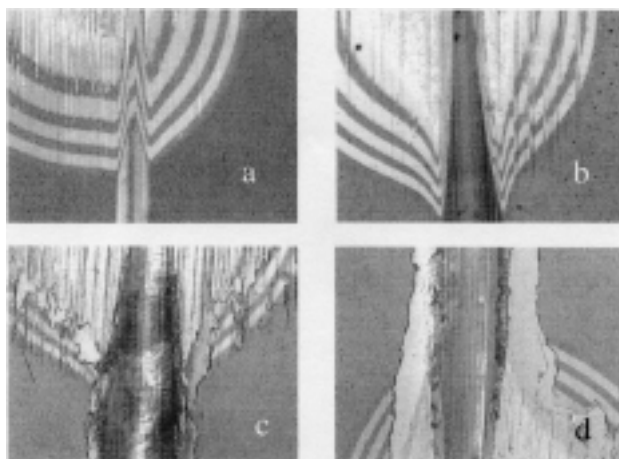


Figure 5: Reflected-light micrographs of ball craters on the scratch track of a $\text{Ti}_{0.5}\text{Al}_{0.5}\text{N}/\text{CrN}$ multilayer coating on a HSS substrate at normal scratch loads of 23 N (a), 52 N (b), 65 N (c) and 80 N (d). Mag. 140x

Slika 5: Optičnomikroskopski posnetki (140-kratna povečava) krogljnih obrusov na razi, narejeni z diamantno konico med preskusom adhezije; vrednost normalne sile med razenjem je bila 23 N (a), 52 N (b), 65 N (c) in 80 N (d)

critical loads for the $\text{Ti}_{0.5}\text{Al}_{0.5}\text{N}/\text{CrN}$ multilayer are much higher than those for the $\text{Ti}_{0.5}\text{Al}_{0.5}\text{N}$ single layers. The failure mode of the multilayer coating results from substrate-coating interfacial detachment and no failure was observed at the CrN-TiAlN interfaces.

The ball-crater preparation technique was used on the scratch tracks to observe the deformation and fracture behaviour (**Figure 5**). For loads lower than 55 N only plastic deformation without any visible failure was observed (**Figures 5a, b**). Beginning at loads greater than 60 N, cracking through the whole layer was observed as the coatings were bent into the scratch track and chipping of the coating occurred on both sides of the scratch track (**Figure 5c**). At loads between 70 and 80 N the coating in the scratch track was completely removed (**Figure 5d**). Around the scratch track the coating was chipped over large areas.

All the samples were oxidized in the temperature range 700-900 °C. CrN coatings began to oxidize at 700 °C, while the oxidation rates of the other two coatings were not significant up to approximately 800 °C. Thermogravimetric measurements of the CrN coating showed that the oxide layer grew according to a parabolic diffusion law. The oxide-layer thickness of the $\text{Ti}_{0.5}\text{Al}_{0.5}\text{N}$ coating initially also increased and followed a parabolic growth. However, after reaching a thickness of approximately 35 nm the oxide growth rate decreased due to the formation of a protective Al-rich oxide layer¹⁵. Thermogravimetric measurements of the $\text{Ti}_{0.5}\text{Al}_{0.5}\text{N}/\text{CrN}$ multilayer coating showed that two main stages of oxidation exist in the temperature range 800-900 °C. For short oxidation times the oxidation rates of the $\text{Ti}_{0.5}\text{Al}_{0.5}\text{N}/\text{CrN}$ and $\text{Ti}_{0.5}\text{Al}_{0.5}\text{N}$ coatings are comparable, and are two times smaller than for CrN. After a long time the oxidation rate of the $\text{Ti}_{0.5}\text{Al}_{0.5}\text{N}/\text{CrN}$ coating is closer to that of the CrN. Using the Arrhenius formula, the activation energies for oxidation (E_a) were determined for all three samples (**Table 1**). The highest value was obtained for $\text{Ti}_{0.5}\text{Al}_{0.5}\text{N}$, while the lowest was for CrN. The coefficients of parabolic oxidation were also determined and their values at 800 °C and 900 °C were compared (**Table 1**). The highest value was obtained for CrN, while the lowest was for $\text{Ti}_{0.5}\text{Al}_{0.5}\text{N}$. The oxide products of the oxidized $\text{Ti}_{0.5}\text{Al}_{0.5}\text{N}/\text{CrN}$ multilayer coating were analyzed by AES depth profiling. **Figure 3** shows AES depth profiles of the as-deposited and partially oxidized $\text{Ti}_{0.5}\text{Al}_{0.5}\text{N}/\text{CrN}$ multilayer coatings. After oxidation at 800 °C the upper oxide layer was rich in Al, while the lower layer was rich in Ti. The X-ray diffraction spectra of the oxidized coatings still showed the peaks of nitride phases, while peaks of the TiO_2 oxide phases were also detected. Owing to the formation of amorphous Al_2O_3 there are no peaks of alumina in the X-ray diffraction patterns. After oxidation at 900 °C the upper oxide layer was rich in Ti, while the lower layer was rich in Cr. The X-ray diffraction pattern at 900 °C is similar to that at 800 °C,

but additional peaks appeared, probably belonging to Al-Cr-O oxide phases. The surface morphology of the partially oxidized samples was analysed by SEM using backscattered electrons and a pronounced and well-developed grain structure was observed. (**Figure 1b**). An SEM micrograph of the fractured cross-section of the sample oxidized at 850 °C for 1300 min shows that the multilayer structure was not destroyed. An AES depth profile of the same sample shows a large increase of the interfacial region, mainly due to the increase in the roughness.

4 CONCLUSIONS

Ti_{0.5}Al_{0.5}N/CrN multilayer coatings were prepared by sputter deposition at a low deposition temperature. The microhardness and Young's modulus of the Ti_{0.5}Al_{0.5}N/CrN multilayered coatings were found to be slightly higher than those observed for the single-layered CrN and TiAlN coatings. All the other properties were halfway between the CrN and the TiAlN. The ball-crater technique used on the scratch tracks showed that the Ti_{0.5}Al_{0.5}N/CrN multilayer structure seems to have very promising elastic-plastic properties. On the basis of these results we can conclude that a multilayer structure seems to be beneficial for some of the mechanical properties of the Ti_{0.5}Al_{0.5}N/CrN hard coating, and as a result this coating has the potential to be a tribological coating material.

ACKNOWLEDGEMENTS

This work was supported by the Ministry of Education Science and Sport of the Republic of Slovenia.

5 REFERENCES

- ¹ S. A. Barnett, *Physics of thin films* (ed. by M. H. Francombe and J. L. Vossen), Academic Press, New York, 1993, 1-77
- ² S. J. Bull, A. M. Jones, *Surf. Coat. Technol.*, 78 (**1996**) 173-184
- ³ W. D. Sproul, *J. Vac. Sci. Technol. A* 12 (**1994**) 4, 1595-1601
- ⁴ H. Holleck, V. Schier, *Surf. Coat. Technol.* 76-77 (**1995**) 328-336
- ⁵ M. Nordin, M. Larsson, S. Hogmark, *Surf. Coat. Technol.*, 106 (**1998**) 234-241
- ⁶ M. Okumiya, M. Griepentrog, *Surf. Coat. Technol.*, 112 (**1999**) 123-128
- ⁷ Q. Luo, W. M. Rainforth, L. A. Donohue, I. Wadsworth, W. D. Munz, *Vacuum* 53 (**1999**) 123-126
- ⁸ I. Wadsworth, I. J. Smith, L. A. Donohue, W. D. Munz, *Surf. Coat. Technol.* 94-95 (**1997**) 315-321
- ⁹ Y. L. Su, W. H. Kao, *Wear* 223 (**1998**) 119-130
- ¹⁰ P. Yashar, S. A. Barnett, J. Rechner, W. D. Sproul, *J. Vac. Sci. Technol. A* 16 (1998) 5, 2913
- ¹¹ M. Larsson, P. Hollman, P. Hedenquist, S. Hogmark, U. Wahlstrom, L. Hultman, *Surf. Coat. Technol.* 86-87 (**1996**) 351-356
- ¹² M. Larsson, M. Bromark, P. Hedenquist, S. Hogmark, *Surf. Coat. Technol.* 91 (**1997**) 43-49
- ¹³ P. Panjan, B. Navinšek, A. Cvelbar, A. Zalar, J. Vlcek, *Surf. Coat. Technol.* 98 (**1998**) 1497-1502
- ¹⁴ M. Ohring, *The material science of thin films*, New York, Academic Press, 1992, 416
- ¹⁵ P. Panjan, B. Navinšek, M. Čekada, A. Zalar, *Vacuum*, 53 (**1999**) 127-131

